Available online at www.sciencedirect.com
SCIENCE DIRECT®
Journal of Molecular Catalysis A: Chemical 208 (2004) 175–185
JOURNAL OF MOLECULAR CATALYSIS A: CHEMICAL
www.elsevier.com/locate/molcata

Characterization of acylating intermediates formed on H-ZSM-5

O. Kresnawahjuesa [a], R.J. Gorte [a,*], David White [b]

[a] *Department of Chemical and Biomolecular Engineering, University of Pennsylvania, Philadelphia, PA 19104, USA*
[b] *Department of Chemistry, University of Pennsylvania, Philadelphia, PA 19104, USA*

Received 9 July 2003; received in revised form 9 July 2003; accepted 10 July 2003

Abstract

The adsorption of typical acylating agents (acetic acid, acetic anhydride and acetyl chloride) on the Brønsted-acid sites in H-ZSM-5 has been investigated with temperature-programmed-desorption (TPD) and thermogravimetric analysis (TGA), infrared spectroscopy and ^{13}C NMR. Acetic acid forms a hydrogen-bonded complex with the Brønsted sites that is characterized by ν(C–H) stretching frequencies of 1740 and 1750 cm^{-1}. Both acetyl chloride and acetic anhydride react with the Brønsted sites below 400 K, forming an acetyl-zeolite intermediate and either HCl or acetic acid, characterized by a ν(C–H) stretching frequency of 1705 cm^{-1}. The acetyl-zeolite intermediate reacts readily at room temperature with either water (forming acetic acid) or ammonia (forming acetamide). ^{13}C NMR isotropic shifts for the C-2 carbon of the acetic-acid adsorption complex and the acetyl-zeolite intermediate occur at similar frequencies, making them difficult to distinguish by this technique. In TPD, the acetyl-zeolite intermediate decomposes, with CO_2 and acetone being the primary initial products. Most of acetic acid desorbs unreacted, although a fraction also forms CO_2 and acetone, suggesting the formation of an acetate intermediate at higher temperatures. The implications of results for understanding acylation reactions on zeolites are discussed.

Keywords: Friedel-Craft acylation; Zeolite; Acetic acid; Acetyl chloride; Acetic anhydride; Acetyl-zeolite intermediate

1. Introduction

Zeolite, solid–acid catalysts have shown potential to replace homogenous catalysts for synthesizing aromatic ketones via Friedel-Craft acylation reactions and the related Fries rearrangement of aromatics [1,2]. The traditional method for preparing these aromatic ketones involves reaction of the hydrocarbon with carboxylic acid derivatives using a solid Lewis-acid or a solution-phase Brønsted-acid. The major problem with these traditional approaches is the requirement of using a stoichiometric quantity of acid relative to the formed ketone. In the case of a Lewis-acid, the reaction products (ketones) form a stable complex with the acid sites. The product recovery is generally carried out with water, which results in the total destruction of the catalyst, generating a great deal of corrosive and toxic waste products [1].

Despite the potential that heterogeneous solid–acid catalysts show for acylation reactions [3–6], there are problems that prevent the utilization of these catalysts universally. Usually, heterogeneous catalysts show poor activity and poor selectivity with respect to the desired products. Also, catalyst deactivation due to coking or strong adsorption of one of the reactants or products is frequently observed [6].

One problem with applying heterogeneous catalysts to many of these reactions is that the chemistry at the acid sites is not well understood. The typical approach for developing a new process with solid acids involves reactor studies where a variety of catalysts are tested under a wide range of conditions. It is true that this approach must be taken as a final step, but there are many experimental variables (type of catalyst, temperature, partial pressures, reactant compositions, etc.) that need to be considered. Without insights into the interaction of typical reactants or products with the active sites on the molecular level, it is very difficult to determine the reason why a particular reaction fails. More importantly, understanding how typical acylating agents interact with the active sites can provide alternative strategies for achieving the best combination of catalyst and reaction conditions.

In this paper, the nature of interactions between typical acylating agents with the acid sites in H-ZSM-5 have been investigated with temperature-programmed-desorption

* Corresponding author. Tel.: +1-215-898-8351; fax: +1-215-573-2093.
E-mail address: gorte@seas.upenn.edu (R.J. Gorte).

1381-1169/$ – see front matter © 2003 Elsevier B.V. All rights reserved.
doi:10.1016/S1381-1169(03)00511-9

(TPD)–thermogravimetric analysis (TGA), diffuse reflectance FTIR, and solid-state NMR in an attempt to provide chemical intuition that might be useful for investigating acylation reactions. The zeolite H-ZSM-5 was chosen for study since the Brønsted-acid sites in this material are well defined and characterized [7]. When properly prepared, the Brønsted-acid site density in this material has been shown to be equal to the framework Al concentration. Furthermore, the reaction rates for *n*-hexane cracking, xylene isomerization, propylene polymerization, methanol-to-olefins reaction, toluene disproportionation, and cumene cracking were shown to linearly increase with Al content in H-ZSM-5 [8]. Researchers at Mobil also performed Cs-poisoning studies to show that all framework-Al sites contribute a strong Brønsted site [9]. Since one would expect each Cs ion to preferentially poison the strongest sites first, the observation that the activity of partially exchanged materials decreases linearly with Cs content, with a stoichiometry of one Cs/Al required to eliminate the activity, suggests the activity of each site in H-ZSM-5 is essentially identical.

The advantage of working with a material that has essentially identical sites is that most spectroscopic methods tend to provide information that is "averaged" over all sites. Since all sites are catalytically equivalent in H-ZSM-5, the spectroscopic data can be immediately applied to understanding the nature of species that will be present under reaction conditions. It is unlikely that minority sites, not observed in the spectroscopic measurements, would be responsible for most of the chemistry.

2. Experimental

The Al-containing zeolite used in this study was a standard reference sample obtained from NIST and reported to have Si/Al_2 ratio of 60. It was obtained in the ammonium-ion form and simply calcined in flowing air at 773 K to convert it into the protonic (H-ZSM-5) form. The Brønsted-acid site concentration was determined from TPD–TGA of isopropylamine to be 500 μmol/g. In isopropylamine TPD–TGA measurements, the site density is determined from amount of isopropylamine that decomposes into propylene (m/e = 41) and ammonia (m/e = 17) between 575 and 650 K [10–13]. The site density obtained from this measurement agrees well with the reported framework Al concentration.

The TPD–TGA studies were carried out using a Cahn 2000 microbalance attached to an ultra-high vacuum chamber equipped with a quadrupole mass spectrometer. The system could be evacuated with turbomolecular pump and had a base pressure below 1×10^{-7} Torr. Between 20 and 30 mg of sample were spread thinly over the flat sample pan of the microbalance to minimize bed effects during adsorption and desorption [13]. The heating rate was 10 K/min in all cases. During the desorption event, the desorbing species were monitored using the entire mass range from $m/e = 1$ to 100 of the mass spectrometer to identify products from the entire fragmentation pattern. For those cases where discrimination of molecules was difficult using the mass spectrometer, the desorption products were trapped with a liquid-N_2 cold finger and analyzed using a gas chromatograph with an FID detector, as described elsewhere [14].

In all of the adsorption measurements, the sample was exposed to the vapor pressure of the adsorbate at 295 K. It was possible to control the initial uptake of molecules on the zeolite by controlling the exposure, and this was found to be crucial for some experiments due to secondary reactions between molecules adsorbed on the Brønsted sites and additional molecules in the zeolite. The TPD–TGA measurements were obtained following evacuation of the samples for 45 min to remove some of the weakly adsorbed species. Varying the evacuation time only affected the TPD–TGA results by changing the amount of weakly adsorbed species desorbing at low temperature.

The NMR spectrometer has been described elsewhere [15]. The static spectra were obtained at a field of 3.5 T (37.48 MHz ^{13}C resonance frequency) and the line shapes were determined from the observation of proton-decoupled Hahn Echoes. The echo sequence consisted of a series of 90°–*t*–180°–*t* pulses, in quadrature, with a delay time, *t*, of 70 μs. For the NMR measurements, approximately 130–150 mg of H-ZSM-5 were degassed at 700 K and 10^{-6} Torr for 24 h. The degassed samples were exposed to controlled amounts of isotopically labeled, carbonyl (C-2) ^{13}C of acetic acid ($CH_3{}^{13}COOH$), acetic anhydride ($(CH_3{}^{13}CO)_2O$), or acetyl chloride ($CH_3{}^{13}COCl$) obtained from Cambridge Isotope Labs, Inc. using a calibrated volume. To avoid bed effects in adsorption, the zeolite was spread thinly along the length of an evacuated, 1/2 in. tube during exposure to the adsorbate and then transferred into a smaller tube without exposure to air. The smaller tube was sealed with a torch and inserted into a home-built, double-resonance, static NMR probe. In all cases, the spin-counting measurements agreed with the measured dosing volumes. In some cases, the sealed sample was opened under a N_2 environment to release the gas-phase molecules formed during the high-temperature treatment.

The FTIR spectra were collected on a Mattson Galaxy FTIR with a diffuse reflectance attachment (Spectra-Tech Inc., Collector II). The system allowed measurements to be performed at temperatures ranging from room temperature to 800 K in flowing, dry N_2, before and after exposing the sample to the adsorbate of interest.

3. Results

3.1. TPD–TGA measurements

TPD–TGA results for acetic acid on H-ZSM-5 are shown at Fig. 1 following a controlled exposure to a coverage near one molecule/site. The small amount of weakly adsorbed acetic acid (m/e = 60) leaving the sample below 400 K,

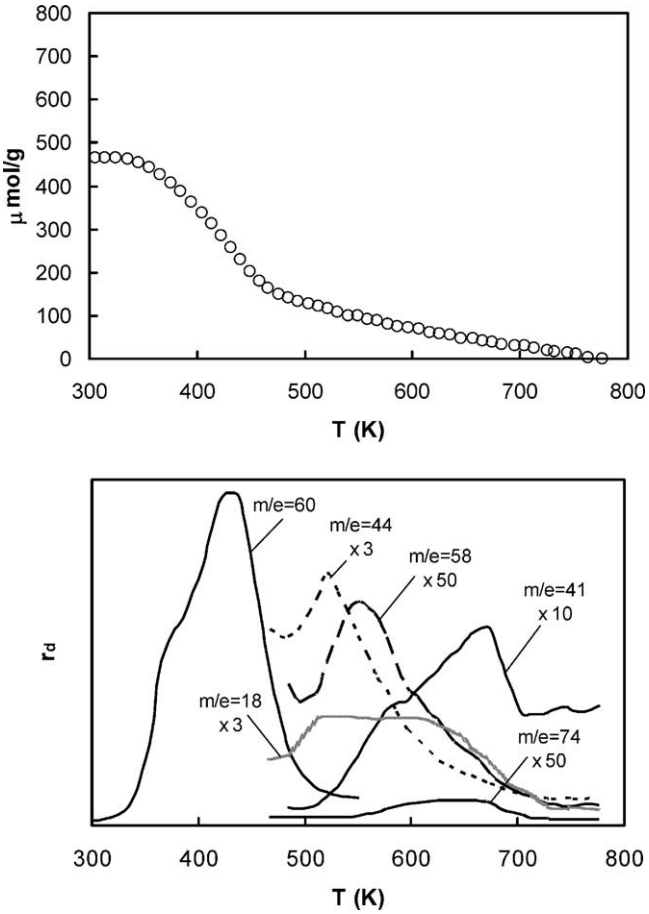

Fig. 1. TPD–TGA results for acetic acid on H-ZSM-5 following controlled exposure at 298 K. The TPD peaks correspond to water ($m/e = 18$), unreacted acetic acid ($m/e = 60$), CO_2 ($m/e = 44$), acetone ($m/e = 58$), propylene ($m/e = 41$) and C6 hydrocarbons ($m/e = 74$).

observed as an inflection point in the $m/e = 60$ peak, is associated with non-acidic sites or with molecules adsorbed on occupied sites, since the amount desorbing between 300 and 400 K increases significantly when the coverage is increased above one molecule/site. Even for the molecules that are hydrogen-bonded to the Brønsted sites, most desorb unreacted between 400 and 500 K, with only one third leaving the sample as other products above 500 K. The mass spectra indicate that two of the major desorbing species are CO_2 ($m/e = 44$) and acetone ($m/e = 58$), and the formation of these products was further confirmed by GC analysis of the products trapped between 500 and 600 K. Based on the fact that CO_2 and acetone are formed by decomposition of the acetyl-zeolite intermediate, to be discussed shortly, we believe that formation of water at higher temperatures is associated with the formation of this intermediate,

$$CH_3COOH + H^+ \cdots ZO^- \leftrightarrow CH_3CO^+ \cdots ZO^- + H_2O \quad (1)$$

and the formation of CO_2 and acetone are associated with the decomposition of acetyl-zeolite intermediate, to be discussed shortly. However, the acid catalyzed decomposition of acetic acid shown in Reaction 2 could also responsible for the formation of these molecules [16,17].

$$2CH_3COOH \rightarrow CO_2 + CH_3COCH_3 + H_2O \quad (2)$$

Whichever mechanism is responsible for CO_2 and acetone, it is clear that only a fraction of the acetic acid reacts and that this reaction occurs at higher temperatures. At still higher temperatures, above 600 K, the TPD shows a wide range of hydrocarbon products (from C-2 to C-8), although a more careful analysis by GC shows that the majority of the desorbing species were propylene ($m/e = 41$) and C-6 hydrocarbons ($m/e = 74$). The formation of propylene and carbon dioxide can be attributed to thermal decomposition of acetic acid, a reaction that has been observed in many geological studies [18]. The formation of C-6 compounds is due to the oligomerization of either acetone or propylene in the presence of acid sites above 500 K [19–24].

The TPD–TGA results following exposures of acetyl chloride and acetic anhydride to H-ZSM-5 are shown in Figs. 2 and 3. For both acetyl chloride and acetic anhydride, the results indicate that an acetyl-zeolite intermediate is formed

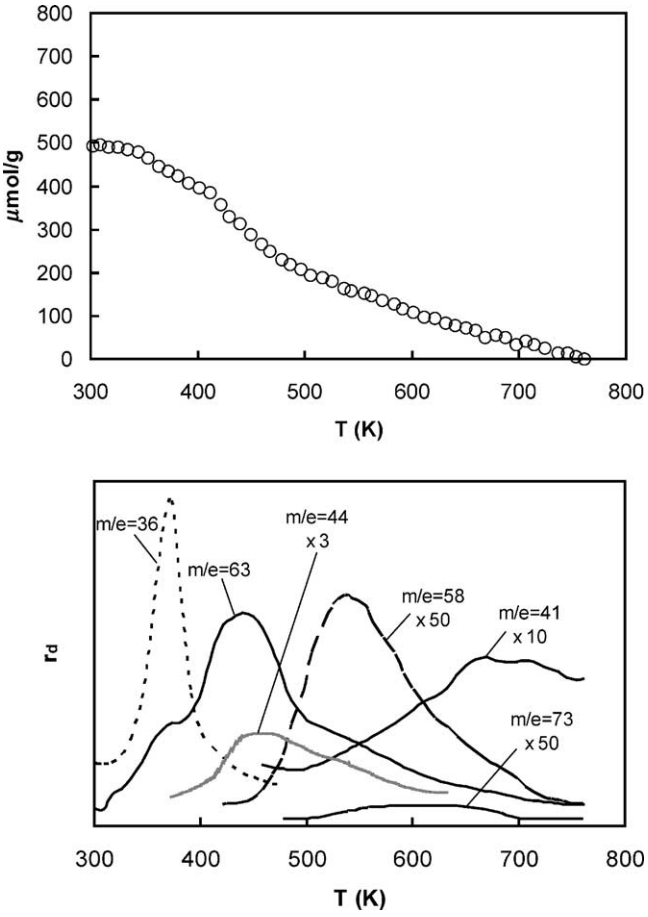

Fig. 2. TPD–TGA results for acetyl chloride on H-ZSM-5 following controlled exposure at 298 K. The TPD peaks correspond to HCl ($m/e = 36$), unreacted acetyl chloride ($m/e = 63$), CO_2 ($m/e = 44$), acetone ($m/e = 58$), propylene ($m/e = 41$) and C6 hydrocarbons ($m/e = 73$).

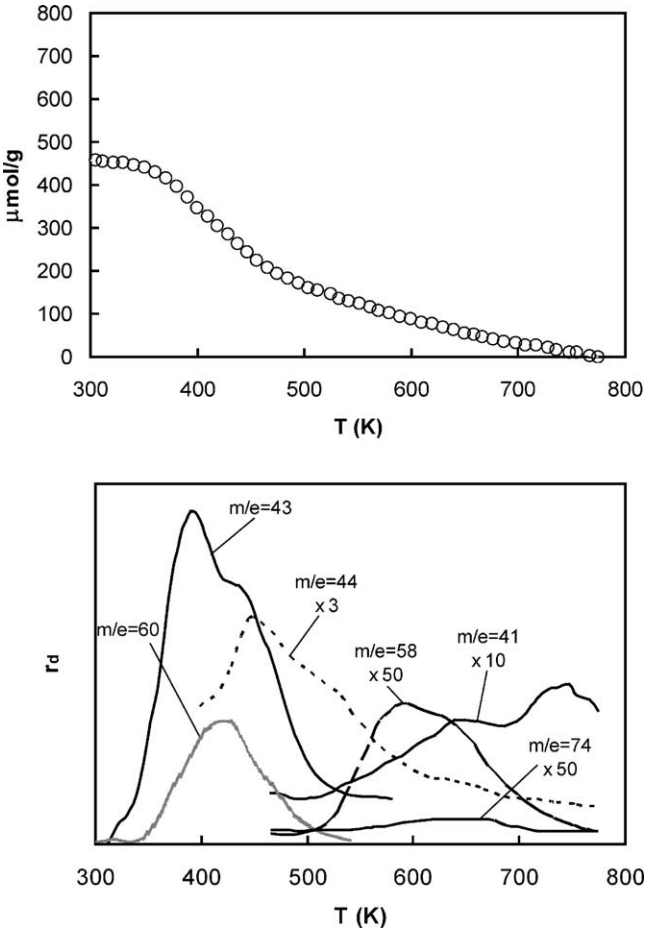

Fig. 3. TPD–TGA results for acetic anhydride on H-ZSM-5 following controlled exposure at 298 K. The TPD peaks correspond to acetic acid ($m/e = 60$), unreacted acetic anhydride ($m/e = 43$), CO_2 ($m/e = 44$), acetone ($m/e = 58$), propylene ($m/e = 41$) and C6 hydrocarbons ($m/e = 74$).

in the zeolite above 373 K. In these experiments, the exposure was again controlled to obtain an initial coverage of ~1 molecule/site to minimize secondary chemistry. Considering first the results for acetyl chloride in Fig. 2, the formation of the acetyl-zeolite intermediate zeolite ($CH_3CO^+ \cdots ZO^-$) is demonstrated by the production of HCl ($m/e = 36$) according to Reaction 3:

$$CH_3COCl + H^+ \cdots ZO^- \leftrightarrow CH_3CO^+ \cdots ZO^- + HCl \quad (3)$$

Based on the mass changes, it appears that approximately two thirds of the initially adsorbed acetyl chloride reacted, leaving one third, 150 μmol/g, to desorb intact. This unreacted acetyl chloride ($m/e = 63$) leaves the sample between 400 and 500 K. Also desorbing between 400 and 600 K is CO_2 ($m/e = 44$), which is probably a product of the bi-molecular reaction of the acetyl-zeolite intermediate (Reaction 4). Obviously, the bimolecular reaction requires desorption of the intermediate from the acid sites, probably as ketene (Reaction 5). Propylene, the other product of Reaction 3, reacts further with ketene to form acetone ($m/e = 58$) and acetylene (Reaction 6). The TPD data show that acetone desorbs between 500 and 700 K, while acetylene cannot be observed due to its high reactivity at this temperature [21].

$$2CH_3CO^+ \cdots ZO^- \rightarrow CO_2 + C_3H_6 \quad (4)$$

$$CH_3CO^+ \cdots ZO^- \leftrightarrow CH_2CO + H^+ \cdots ZO^- \quad (5)$$

$$C_3H_6 + CH_2CO \rightarrow CH_3COCH_3 + C_2H_2 \quad (6)$$

As with acetic acid, hydrocarbon products ranging from C-2 to C-8 were detected between 500 and 750 K; again the predominant products are propylene ($m/e = 41$) and C-6 hydrocarbons ($m/e = 74$).

The adsorption chemistry for acetic anhydride, including the formation of acetyl-zeolite intermediate, is very similar to that found with acetyl chloride. Fig. 3 shows a TPD–TGA measurement following adsorption of acetic anhydride on H-ZSM-5 at a coverage ~1 molecule/site. Some of the acetic anhydride ($m/e = 43$) desorbs unreacted below 400 K. While the intensity of this peak in the mass spectrum is high, the gravimetric results indicate that the amount that leaves the sample unreacted is relatively small. Above ~400 K, significant amounts of acetic acid ($m/e = 60$ and 43) are detected. Since the fragmentation patterns for acetic acid and acetic anhydride are similar, the formation of these products was confirmed by GC analysis.

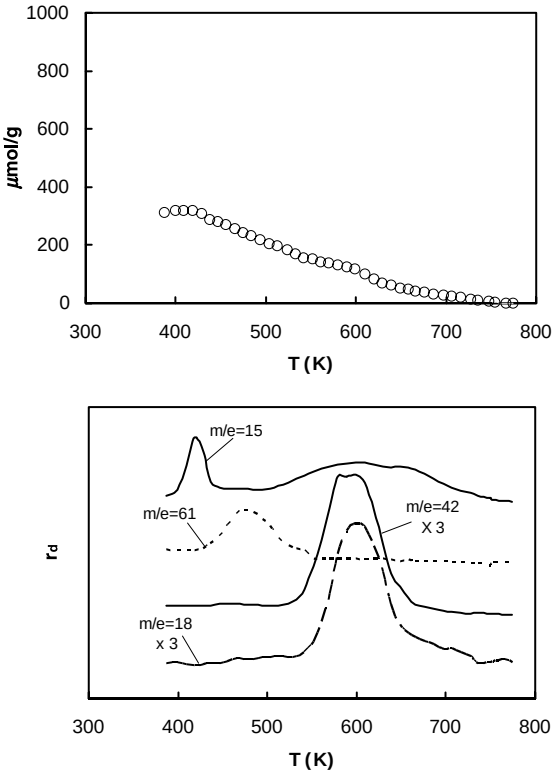

Fig. 4. TPD–TGA results on H-ZSM-5 after exposure to acetyl chloride at 383 K, followed by ammonia. Unreacted ammonia ($m/e = 15$) desorbs from the sample initially. Formation of acetamide ($m/e = 61$) from 430 to 530 K implies the formation of acetyl-zeolite. The acetamide which associated with Brønsted site decomposes to acetonitrile ($m/e = 42$) and water ($m/e = 18$) from 550 to 650 K.

The production of acetic acid implies formation of the acetyl-zeolite intermediate, as shown in Reaction 6:

$$(CH_3CO)_2O + H^+ \cdots ZO^- \leftrightarrow CH_3CO^+ \cdots ZO^- + CH_3COOH \quad (7)$$

Again, the formation of CO_2 ($m/e = 44$) above 400 K and the formation of acetone ($m/e = 58$) above 500 K are similar to the chemistry observed for the acetyl-zeolite intermediate formed by the adsorption of acetyl chloride (Reactions 4 through 6).

To further substantiate whether the intermediate formed by acetyl chloride is consistent with the acetyl-zeolite intermediate, we exposed it to ammonia and looked for the formation of acetamide. In these measurements, the zeolite was again exposed to acetyl chloride to a coverage of ~1 molecule/site and then heated to 373 K in vacuum to remove the by-product HCl. Finally, the sample was exposed to ammonia and a TPD–TGA measurement was performed, with the results shown in Fig. 4. A small amount of NH_3 ($m/e = 15$) is observed at the beginning of the temperature ramp, followed by a small amount of acetamide ($m/e = 61$) between 400 and 500 K. We assign this initial acetamide formation to the reaction between ammonia and excess acetyl chloride not present at the acid sites. The majority of the product desorbs as acetonitrile ($m/e = 42$) and water ($m/e = 18$). Based on earlier work [24], the decomposition feature between 550 and 700 K is due to the reaction of protonated acetamide at Brønsted sites in H-ZSM-5.

$$CH_3CONH_3 \cdots ZO^- \rightarrow CH_3CN + H_2O + H^+ \cdots ZO^- \quad (8)$$

It is interesting to notice that the dehydration of the protonated acetamide occurs at essentially the same temperature at which the decomposition of protonated amines react via the Hoffman elimination [10–12].

3.2. FTIR measurements

Infrared spectroscopy was employed to investigate the nature of acetic acid and acetyl chloride adsorption in the zeolite. The data for acetic acid are shown in Fig. 5. Because we were unable to control exposure to the sample in the FTIR measurements, all measurements started from high initial coverages and lower coverages were obtained by heating and flushing the sample with inert, dry N_2. The spectrum in Fig. 5a) is that of H-ZSM-5 before exposure.

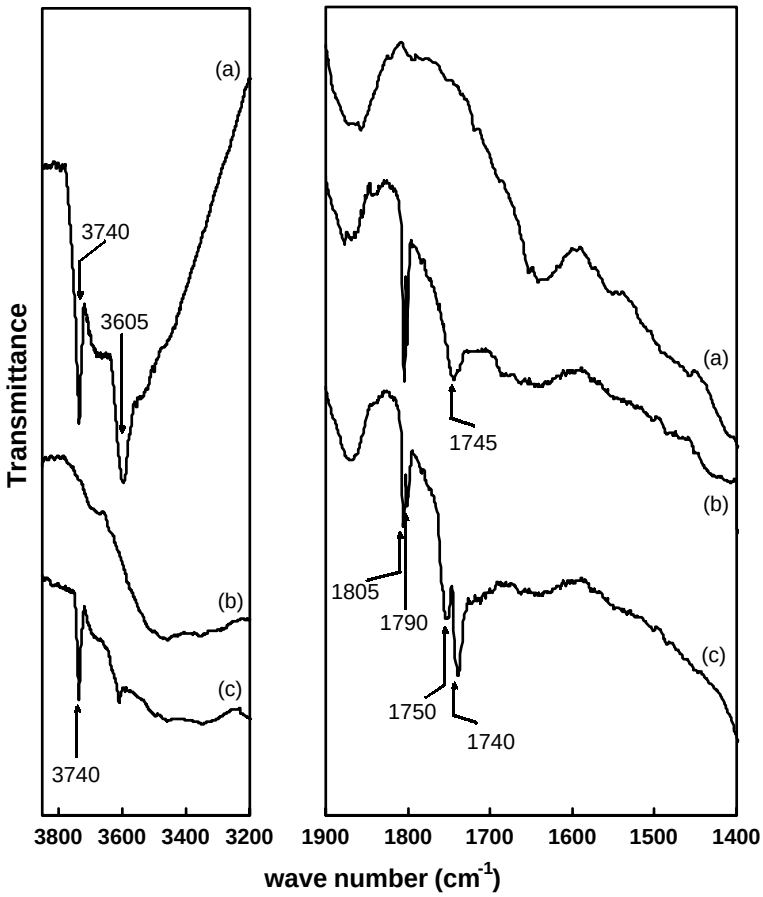

Fig. 5. Diffuse reflectance FTIR spectra of the following samples: (a) clean H-ZSM-5 at 473 K; (b) H-ZSM-5 after exposure to acetic acid, followed by flushing with dry N_2 at 298 K; and (c) heat (b) to 373 K followed by flushing with dry N_2.

The peak at 3605 cm^{-1} is due to the Brønsted-acid hydroxyls associated with framework Al sites, while the peak at 3740 cm^{-1} indicates the presence of hydroxyl defects or terminal silanols in the H-ZSM-5 sample. Fig. 5b) shows the H-ZSM-5 sample after it had been saturated with the acetic acid at room temperature, followed by flushing with inert, dry N_2. The coverage of acetic acid was obviously very high since both the acidic hydroxyls and the terminal silanols are strongly perturbed. The presence of weakly adsorbed acetic acid is also indicated by the symmetric and anti-symmetric carbonyl stretches at 1805 and 1790 cm^{-1}. These frequencies are close to that observed for gas- and liquid-phase acetic acid. A relatively small, broad feature at 1745 cm^{-1} is due to acetic acid molecules that are interacting strongly with Brønsted-acid sites, as will be shown in the subsequent discussion. Upon heating the sample to 373 K, Fig. 5c, some of the weakly adsorbed acetic acid is removed from the sample, as shown by the reappearance of the silanol peak at 3740 cm^{-1}. The peaks corresponding to the hydrogen-bonded species at Brønsted-acid sites also increase significantly in relative intensity and separate into two bands. Even though some weakly adsorbed acetic acid is removed by this heating, the presence of peaks at 1805 and 1790 cm^{-1} indicate that complete removal of these species were difficult.

The carbonyl stretching frequencies observed for acetic acid in H-ZSM-5 provide important insights into the nature of the bonding. For acetic acid that is fully protonated by fluorosulphonic acid, the carbonyl stretches occur at 1615 and 1560 cm^{-1} [25]. The shift to 1750 and 1740 cm^{-1} for molecules adsorbed at Brønsted sites H-ZSM-5 is therefore consistent with the formation of a relatively strong hydrogen bond, but not proton transfer.

Fig. 6 shows IR spectra of acetyl chloride on H-ZSM-5, with the clean H-ZSM-5 shown again in Fig. 6a and b is the spectrum obtained after exposure to acetyl chloride at 373 K. As with acetic acid, the disappearance of both the acidic hydroxyls and the silanol peaks in the spectrum indicate that the coverage is well above one per acid site. Peaks at 1900 and 1810 cm^{-1} are associated with the ν(C–Cl) and ν(C=O) stretches of weakly adsorbed acetyl chloride. More interestingly, a new feature at 1705 cm^{-1} appeared, which we assign to the ν(C=O) stretch of the acetyl-zeolite intermediate. The spectrum obtained after heating the sample to 423 K, Fig. 6c, shows that the weakly adsorbed species has been removed, while the acetyl-intermediate peak at 1705 cm^{-1}

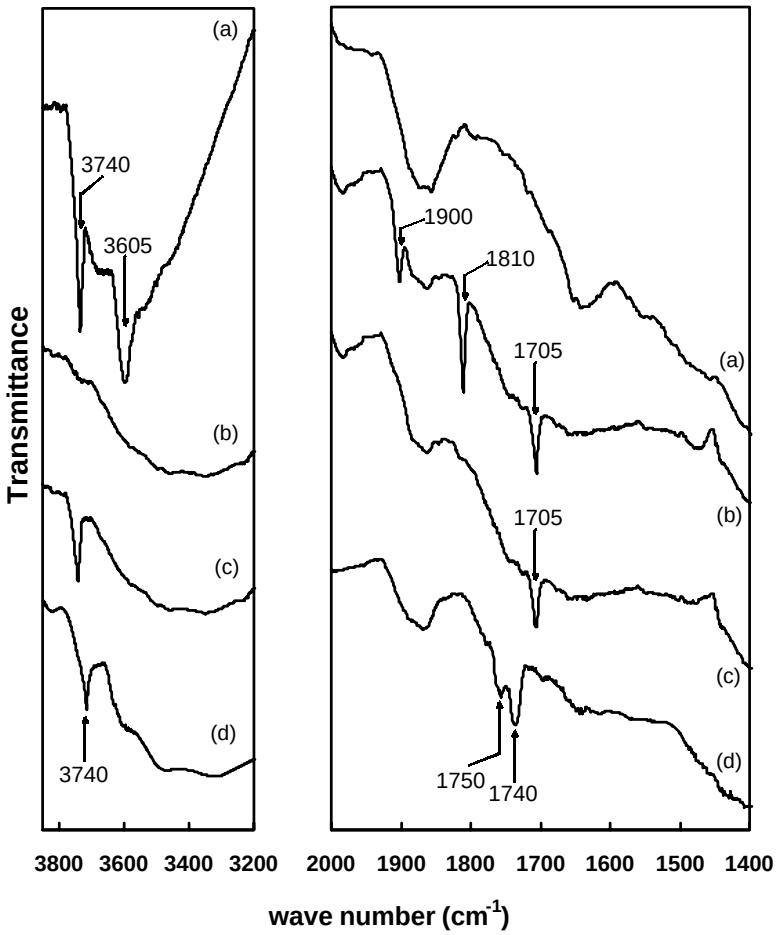

Fig. 6. Diffuse reflectance FTIR spectra of the following samples: (a) clean H-ZSM-5 at 473 K; (b) H-ZSM-5 after exposure to acetyl chloride at 373 K followed by flushing with dry N_2; (c) heat (b) further to 423 K; and (d) exposed (c) to water to produce hydrogen-bonded acetic acid at 423 K.

remains. It is noteworthy that the ν(C=O) stretching frequency of the intermediate is somewhat lower than that observed for organic-acetate esters. Propyl and butyl acetate are reported to have a carbonyl stretching frequency of 1760 cm^{-1} [26]. The lower frequency of the zeolite ester would suggest that the C=O bond is weakened relative to normal esters.

Finally, the consistency of the assignments in Figs. 5 and 6 are shown by the result in Fig. 6d, which was obtained after exposing the sample in Fig. 6c to water vapor at 423 K. After exposure to water, the acetyl-intermediate peak at 1705 cm^{-1} disappears and is replaced by peaks at 1750 and 1740 cm^{-1}, which we have previously assigned as being due to hydrogen-bonded acetic acid. Consistent with this assignment, the peak at 3605 cm^{-1}, due to Brønsted sites, has not reappeared. Unlike the spectra obtained after exposing the Brønsted sites to acetic acid, no weakly adsorbed acetic acid is present, as indicated by the absence of bands at 1805 and 1790 cm^{-1}. Since all of the acetyl-zeolite intermediates should be associated with acid sites, this observation is again consistent with the chemistry that has been proposed.

3.3. ^{13}C NMR measurements

To further characterize the nature of the adsorbed species, ^{13}C NMR measurements of acetic acid, acetyl chloride, and acetic anhydride were performed in H-ZSM-5. Fig. 7 shows the static NMR spectra of carbonyl (C-2) ^{13}C of acetic acid ($CH_3{}^{13}COOH$) at coverages of 0.3, 0.8, 1.4 and 2.0 molecule per site following adsorption at room temperature. The spectra show that the carbonyl (C-2) ^{13}C peak for acetic acid gradually shifts from 188 to 182 ppm with increasing coverage. For comparison, the isotropic shift for the C-2 carbon of the carbonyl carbon of acetic acid is 177 ppm [27]. Also, the peaks narrow with increasing coverage, starting with a peak width of 1.4 kHz at the lowest coverage and decreasing to 0.4 kHz at the highest coverage. The decreasing peak width is clear evidence for exchange processes, which we associate with weakly adsorbed molecules or the presence of more than one molecule per site. As we have already pointed out, there is a great deal of evidence that sites in H-ZSM-5 are essentially equivalent; therefore, it appears that acetic acid molecules associated with the Brønsted sites at a 1:1 coverage exhibit an isotropic shift of 188 ppm, with more weakly adsorbed molecules exhibiting shifts at lower values. The isotropic shifts that we have observed are in the range typically reported for the carbonyl (C-2) ^{13}C labeled acetic acid in various solid salts [28]. The chemical shift we ascribe to the 1:1 species for acetic acid is somewhat higher than the value observed by van Bekkum and co-workers [29], who reported a chemical shift of 182 ppm at a coverage 0.2 molecule/site for acetic acid carbonyl (C-2) ^{13}C peak in H-ZSM-5.

The spectrum in Fig. 8a was obtained after heating the sample with 1.4 molecules/site to 528 K for 47 h. After heating, the spectrum shows a peak at 19 ppm that can be assigned to the formation of aliphatic carbons that was also observed in the TPD measurements as the oligomers (from C-2 to C-8) which are desorbing at high-temperature. The MAS of sample in Fig. 8a) at 150 K, at spinning frequency of 995 Hz, is shown on Fig. 8b). The resulting chemical shielding tensor implies that a localized acetyl-zeolite intermediate is being formed after heating at 528 K. The zero-order side band (isotropic chemical shift (σ_{iso})) of the adsorption complex, at 183 ppm, is indicated by the arrow. A simulation, performed according to the method described elsewhere [38,39], was used to obtain acetyl-zeolite intermediate principal elements of the carbonyl ^{13}C shielding tensors; $\sigma_{xx} = 287$, $\sigma_{yy} = 177$, and $\sigma_{zz} = 82$.

The spectrum in Fig. 8c was obtained after heating the sample with 1.4 molecule/site, the sample in the spectrum of Fig. 8a), to 528 K for 110 h. After heating, the spectrum shows a narrow peak at 128 ppm that can be assigned to gas-phase $^{13}CO_2$ formed by the decomposition [18] that was also observed in the TPD measurements. Opening the sample to allow the gas-phase products to escape eliminated this peak from the spectrum. The other new peak at 20 ppm can be assigned to the formation of aliphatic carbons.

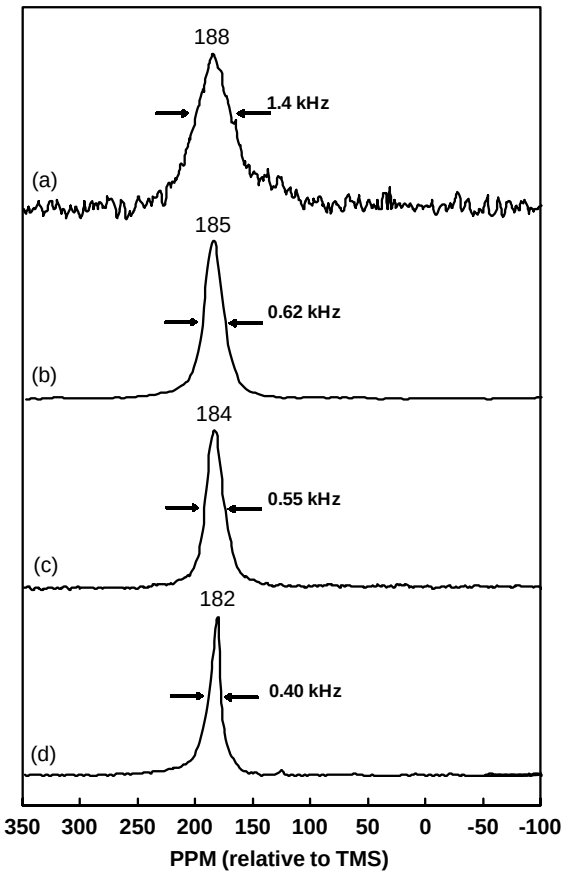

Fig. 7. Static state C-2 ^{13}C NMR of acetic acid ($CH_3{}^{13}COOH$) on H-ZSM-5 at different coverages. (a) 0.3; (b) 0.8; (c) 1.4; and (d) 2.0 molecule/site before heating. HHFW indicates half height line width.

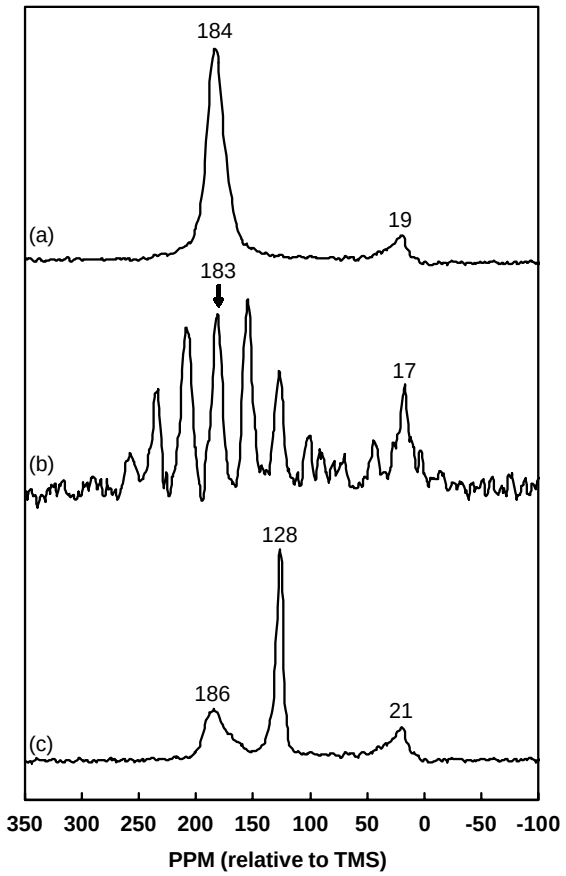

Fig. 8. C-2 ^{13}C NMR of acetic acid ($CH_3{}^{13}COOH$) on H-ZSM-5 at coverage of 1.4 molecules/site. (a) Static state, after heating for 47 h at 528 K; (b) MAS of (a) at 150 K and 995 Hz, $\sigma_{xx} = 287$, $\sigma_{yy} = 177$, $\sigma_{zz} = 82$ and $\sigma_{iso} = 183$ ppm (the arrow indicates the isotropic chemical shift); and (c) static state, after heating (a) for 110 h at 528 K.

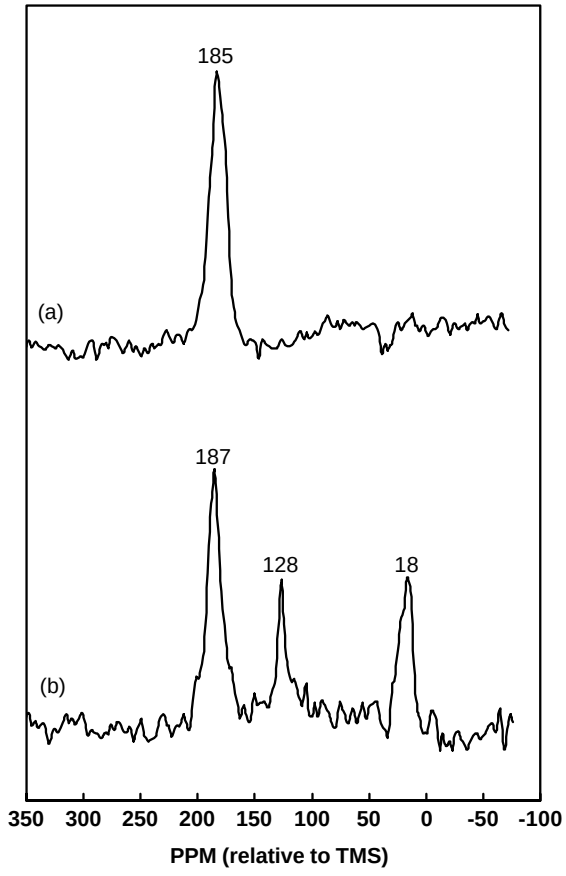

Fig. 9. Static state C-2 ^{13}C NMR of acetyl chloride ($CH_3{}^{13}COCl$) at coverage of 1.4 molecules/site after the following treatment: (a) before heating; and (b) after heating for 17 h at 528 K.

The static, ^{13}C NMR spectra of acetyl chloride ($CH_3{}^{13}COCl$) at a coverage of 1.4 molecules/site and acetic anhydride ($(CH_3{}^{13}CO)_2O$) at coverage 0.9 molecules/site on H-ZSM-5 are shown in Figs. 9 and 10, respectively. These two molecules are similar in that they both form acetyl-zeolite intermediates after heating. Following adsorption at room temperature, the adsorbed carbonyl (C-2) ^{13}C of acetyl chloride shows a peak at 185 ppm (Fig. 9a) while that of acetic anhydride shows a peak at 177 ppm (Fig. 10a). For reference, the isotropic shifts for the carbonyl (C-2) ^{13}C of acetyl chloride and acetic anhydride are reported to be 170 ppm [30] and 166 ppm [27], respectively. The observed shift in frequencies for these molecules in the zeolite is consistent with shifts observed for other carbonyl-containing molecules in liquid acids [31]. Upon heating the samples containing acetyl chloride and acetic anhydride to 528 K, the peak positions for the carbonyl carbon of both molecules shift to 187 ppm; and one again forms CO_2 (128 ppm) and saturated hydrocarbon species (20 ppm). Based on the TPD–TGA and FTIR results, the peak at 187 ppm peak can be assigned, in part, to formation of the acetyl-zeolite intermediate in the zeolite. Since this peak position is the same as that of the 1:1 complex for acetic acid, the isotropic shifts cannot be used to distinguish acetic acid from the acetyl-zeolite intermediate.

The principal elements of the carbonyl ^{13}C shielding tensors obtained from the MAS experiment for acetic acid, acetyl chloride and acetic anhydride together, with its isotropic chemical shift at different conditions, are summarized on Table 1.

It is noteworthy that acetone was not observed in the NMR results, even though this was a major product in the TPD–TGA results. The carbonyl (C-2) ^{13}C of acetone would have been observed at ∼222 ppm if it had been present in significant quantities on the surface [22]. The absence of acetone can be explained in two ways. First, since acetone desorbs below 500 K when it is simply exposed to H-ZSM-5 at room temperature [32], while the acetone formed from the molecules in this study desorbed at much higher temperatures, it would appear that acetone in this study is formed by decomposition of a different surface intermediate. Alternatively, due to the difference in the total pressure above the sample on the TPD–TGA experiment and inside the NMR sealed sample cell, any acetone that

Table 1
Summary of the experimental acetic acid, acetyl chloride and acetic anhydride carbonyl (C-2) ^{13}C shielding tensor and isotropic shift at different conditions

Isotropic shift (ppm)[a] (±5)	$CH_3{}^{13}COOH$					$CH_3{}^{13}COCl$			$(CH_3{}^{13}CO)_2O$		
	95 K (solid)[b]	150 K (unheated) (0.8 molecules/site)	294 K (unheated) (0.8 molecules/site)	150 K (heated) (1.4 molecules/site)	294 K (heated) (1.4 molecules/site)	150 K (unheated) (1.4 molecules/site)	294 K (unheated) (1.4 molecules/site)	294 K (unheated) (1.4 molecules/site)	95 K (solid)[b]	294 K (unheated) (0.9 molecules/site)	294 K (heated) (0.9 molecules/site)
σ_{xx}	268	267		287		263			280		
σ_{yy}	183	195		177		188			115		
σ_{zz}	109	98		82		104			115		
σ_{iso} (MAS)[c]	186	186		183		185			170		
σ_{iso} (static)			185		186		185	187		177	187
σ_{iso} (MAS)			178				170			166	

[a] Relative to isotropic shift of low-pressure, gaseous TMS at room temperature.
[b] Cited from [27].
[c] $\sigma_{iso} = 1/3\mathrm{Tr}(\sigma) = 1/3\ (\sigma xx + \sigma yy + \sigma zz)$.

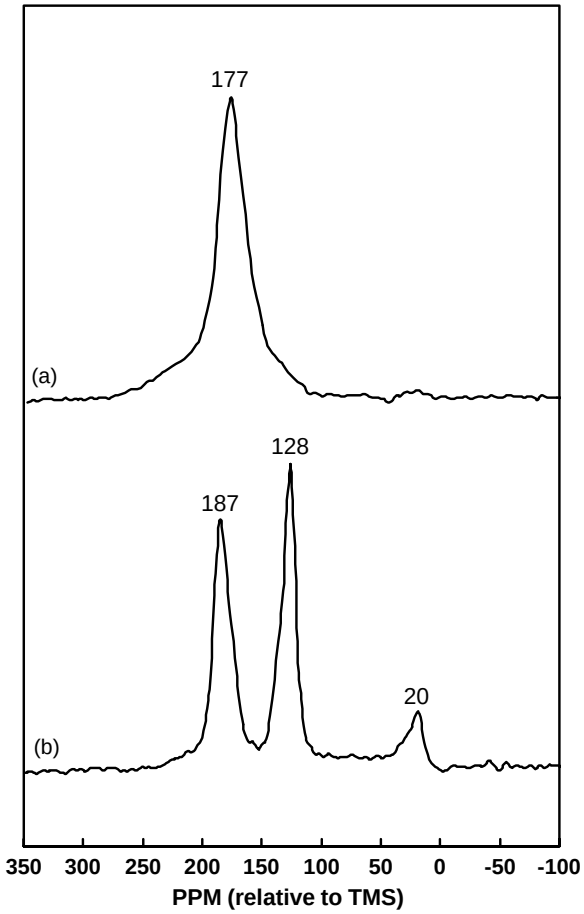

Fig. 10. Static state C-2 ^{13}C NMR of acetic anhydride ($(CH_3{}^{13}CO)_2O$) at coverage of 0.9 molecule/site after the following treatment: (a) before heating; and (b) after heating for 46 h at 528 K.

was formed could have undergone secondary reactions during the sample pretreatment used in the present study. At this point, we cannot distinguish between these possibilities.

4. Discussion

The results from this study demonstrate that acetic acid, acetyl chloride, and acetic anhydride on H-ZSM-5 interact strongly with the Brønsted-acid sites within the zeolite. In the case of acetic acid, the molecules are primarily hydrogen-bonded to the Brønsted sites, as evidenced by the relatively large shift in the carbonyl stretching frequencies. It has been suggested that a 50 cm^{-1} shift in the stretching frequency implies that the molecule is adsorbed primarily through formation of two hydrogen bonds, involving the donation of electron density from the lone-pair orbital of carbonyl carbon to the Brønsted proton [33,34]. In case of acetic anhydride and acetyl chloride, reaction easily occurs at the Brønsted site, forming the acetyl-zeolite intermediate with the zeolite framework. It is noteworthy that the acetyl-zeolite intermediate and acetic acid show similar isotropic chemical shifts in ^{13}C NMR, so that the products and intermediates are not easily differentiated by this technique.

It is interesting to compare the interaction between the Brønsted sites in H-ZSM-5 and acetic acid, acetyl chloride, or acetic anhydride with the adsorption of other polar organic compounds, such as ketones, nitriles, and ethers [32,35]. Based on calorimetric measurements [32] and ^{13}C NMR isotropic shifts [35], it has been argued that molecules having a gas-phase proton affinity equal to or greater than that of ammonia (PA = 858 kJ/mol) are protonated by H-ZSM-5. Molecules that have a proton affinity less than that of ammonia tend to form hydrogen bonds with the Brønsted sites and the strength of the hydrogen bonding appears to vary in a regular manner with the proton affinity of the adsorbate. The proton affinities of acetic acid (PA = 798.4 kJ/mol), acetyl chloride (PA = 739.9 kJ/mol), and acetic anhydride (PA = 827.6 kJ/mol) are clearly less than that of ammonia, but are similar in magnitude to that of simple alcohols, ketones, and ethers. It is therefore not surprising that the molecules examined in this study should behave in a similar manner as the other organic molecules. Considering their proton affinities, the acylating agents examined in this study should be considered strong bases. Similarly, the acylium-ion-like, acetyl-zeolite intermediate that these molecules form is completely analogous to the carbenium-ion-like, alkoxide intermediates formed at Brønsted-acid sites by dehydration of alcohols or protonation of small olefins [40].

Our study has shown that H-ZSM-5 is readily capable of forming acylium-ion-like intermediate that is likely required for the Friedel-Craft, acylation reaction. For acetyl chloride and for acetic anhydride, this intermediate is readily formed at 400 K, well below the typical reaction temperatures that are normally investigated, 450–600 K [2]. Based on our results, we suggest that the reason H-ZSM-5 is often not an effective catalyst for the acylation reaction is not related to the inability of the zeolite to activate these acylating agents. Rather, the problem would appear to be that various other intermediates are formed, such as ketones and olefins. These compounds are well known to produce coke in the zeolite, leading to deactivation of the sites.

If rapid deactivation is indeed the problem [36,37], then the usual approach of looking for solid–acid catalysts that have stronger sites may well be the wrong approach. If deactivation is the limiting issue, one should investigate materials that are less acidic but more resistant to coke formation so as to maintain activity. For example, we have recently demonstrated that the acid sites formed by framework substitution of Fe^{3+} in place of Al^{3+} in the MFI framework leads to Brønsted-acid sites that are less able to promote the hydride-transfer reactions that lead to coke formation during *n*-butene isomerization [14]. Even though H-[Fe]ZSM-5 appears to have weaker sites than H-[Al]ZSM-5, H-[Fe]ZSM-5 is much more resistant to coke formation and showed a similar reaction rate for butane because of this [14]. Similar concepts may prove useful in the development of acylation catalysts.

5. Conclusions

Acetic acid forms strong hydrogen bonds with the Brønsted-acid sites in H-ZSM-5, while acetyl chloride and acetic anhydride react readily with the Brønsted sites to form an acylium-ion-like intermediate. The acetyl-zeolite intermediate is highly reactive and is likely the important intermediate in acylation reactions carried out over zeolite catalysts. Unfortunately, the acetyl-zeolite intermediate decomposes above ∼450 K to products that likely lead to coke formation.

Acknowledgements

This work was supported by the American Chemical Society—Petroleum Research Fund Grant #36615-AC. We are grateful to Dr. Andy I. Biaglow for providing the proton affinity simulation data for various molecules used in this project.

References

[1] P. Metivier, Stud. Surf. Sci. Catal. 130 (2000) 167.
[2] A.K. Pandey, A.P. Singh, Catal. Lett. 44 (1997) 129.
[3] P.B. Venuto, Microporous Mater. 2 (1994) 297.
[4] K. Tanabe, W.F. Holderich, Appl. Catal. A 181 (1999) 399.
[5] A. Corma, Chem. Rev. 95 (1995) 559.
[6] R.S. Downing, H. van Bekkum, R.A. Sheldon, Catal. Technol. (December) (1997) 95.
[7] R.J. Gorte, Catal. Lett. 62 (1999) 1.
[8] D.H. Olson, W.O. Haag, R.M. Lago, J. Catal. 61 (1980) 390.
[9] W.O. Haag, Stud. Surf. Sci. Catal. 84 (1994) 1375.
[10] T.J. Gricus Kofke, R.J. Gorte, W.E. Farneth, J. Catal. 114 (1988) 34.
[11] A.I. Biaglow, C. Gittleman, R.J. Gorte, R.J. Madon, J. Catal. 129 (1991) 88.
[12] C. Pereira, R.J. Gorte, Appl. Catal. A 90 (1992) 145.
[13] W.E. Farneth, R.J. Gorte, Chem. Rev. 95 (1995) 615.
[14] O. Kresnawahjuesa, G.H. Kuhl, R.J. Gorte, C.A. Quierini, J. Catal. 210 (2002) 106.
[15] K.R. Carduner, M. Villa, D. White, Rev. Sci. Instrum. 55 (1984) 68.
[16] Y. Servotte, J. Jacobs, P.A. Jacobs, Proc. Int. Symp. Zeol. Catal., Siofolk (1985) 609.
[17] I. Neves, F. Jayat, P. Magnoux, G. Perot, F.R. Ribeiro, M. Gubelmann, M. Guisnet, J. Mol. Catal. 93 (1994) 169.
[18] P.G. Blake, G.E. Jackson, J. Chem. Soc. B (1969) 94.
[19] J. Novakova, L. Kubelkova, V. Bosacek, K. Mach, Zeolites 11 (1991) 135.
[20] W. Song, J.B. Nicholas, J.F. Haw, J. Phys. Chem. B 105 (2001) 4317.
[21] C. Pereira, G.T. Kokotailo, R.J. Gorte, J. Phys. Chem. 95 (1991) 705.
[22] A.I. Biaglow, J. Sepa, R.J. Gorte, D. White, J. Catal. 151 (1995) 373.
[23] T.J. Gricus Kofke, R.J. Gorte, J. Catal. 115 (1989) 233.
[24] J. Sepa, Ph.D. Thesis, University of Pennsylvania, 1998.
[25] L.M. Parker, Methane Conversion, 1998, p. 589.
[26] http://www.webbook.nist.gov/chemistry.
[27] A. Pines, M.G. Gibby, J.S. Waugh, Chem. Phys. Lett. 15 (1972) 373.
[28] S. Ganapathy, V.P. Chacko, R.G. Bryant, J. Magn. Res. 57 (1984) 239;
S. Ganapathy, V.P. Chacko, R.G. Bryant, J. Chem. Phys. 81 (1984) 661.
[29] V. Bosacek, E.A. Gunnewegh, H. van Bekkum, Catal. Lett. 39 (1996) 57.
[30] J.B. Stothers, P.C. Lauterbur, Can. J. Chem. 42 (1964) 1563.
[31] G.E. Maciel, J.J. Natterstad, J. Chem. Phys. 42 (1965) 2752;
G.E. Maciel, D.D. Traficante, J. Phys. Chem. 69 (1965) 1030.
[32] C.-C. Lee, R.J. Gorte, W.E. Farneth, J. Phys. Chem. B 101 (1997) 3811;
C.-C. Lee, Ph.D. Thesis, University of Pennsylvania, 1996.
[33] L. Kubelkova, J. Cejka, J. Novakova, Zeolites 11 (1991) 48.
[34] M.A. Natal-Santiago, J.M. Hill, J.A. Dumesic, J. Mol. Catal. A 140 (1999) 199.
[35] R.J. Gorte, D. White, Top. Catal. 4 (1997) 57.
[36] F. Richard, H. Carreyre, G. Perot, J. Catal. 159 (1996) 427.
[37] P. Moreau, A. Finiels, S. Pelorgeas, O. Vigneau, M. Lasperas, Catal. Lett. 47 (1997) 161.
[38] M.M. Maricq, J.S. Waugh, J. Chem. Phys. 70 (1979) 3306.
[39] J. Herzfeld, A. Berger, J. Chem. Phys. 73 (1980) 6021.
[40] M.T. Aronson, R.J. Gorte, W.E. Farneth, D. White, J. Am. Chem. Soc. 111 (1989) 840.